1

Introduction

1.1 Overview

Magnetic field sensors have been born and used for many years in early applications of direction finding or navigation. Today, magnetic sensors are still a primary means of navigation, but many more uses have evolved. The technology for sensing magnetic fields has also evolved driven by the need for improved sensitivity, smaller size, and compatibility with electronic systems. The output of other sensors, such as temperature, pressure, strain, and light sensors, directly reports the desired parameters, while using magnetic sensors to detect direction, presence, rotation, angle, or electrical currents only indirectly detect these parameters. The output signal of a magnetic sensor requires some signal processing to translate it into the desired parameter value. This makes magnetic sensing a little more challenging to apply in most applications, but it allows for reliable and accurate sensing of parameters that are difficult to sense otherwise. One approach to the development of magnetic sensors is the pursuit of an ideal device that meets the demands and limitations of all the possible applications. Such an ideal sensor must have an ultra-high resolution, a wide bandwidth, very low power consumption, as well as being miniature, low cost, which, all together, does not seem realistic. An optimal magnetic sensing device is that which best fits a set of requirements dictated by a specific application.

This book aims to assist the readers in their search for their optimal magnetic sensing system. From the more common and popular Hall effect sensors up to the nuclear magnetic resonance (NMR)-based magnetometers, each chapter describes a specific type of sensor and provides useful information that is necessary to understand the magnetometer behavior, including theoretical background, noise model, materials, electronics, applications, design, and fabrication techniques. In this chapter, we outline the history of magnetic sensors, natural and technical magnetic fields, magnetic terms and units, magnetic microsensors and their properties and classification, magnetic sensor

Magnetic Sensors for Biomedical Applications, First Edition. Hadi Heidari and Vahid Nabaei.

Published 2020 by John Wiley & Sons, Inc.

terminology, and noise in magnetic sensors. In Chapter 2, we focus on Hall magnetic sensors, and discuss Hall effect, characteristics of Hall effect devices such as geometry and material, horizontal and vertical CMOS Hall devices, and Hall sensor applications. Magnetoresistance (MR) sensors' material and principles, classes, modeling and simulation, design and fabrication technologies, as well as their various biomedical applications have been outlined in Chapter 3. In Chapter 4, we review models, instruments, and biomedical applications of different resonance magnetometers such as NMR, magnetic resonance imaging, and electron spin resonance. Chapter 5 provides an overview of fundamentals, fabrication technologies, and biomagnetism applications of superconducting quantum interference devices. Comparisons of Hall sensors with other galvanomagnetic sensors, NMR with electron spin resonance, and conclusion are presented in Chapter 6.

1.2 History of Magnetism Studies and of Its Use in Magnetic Sensors

The expression "magnet" or "magnetic" originates from the region Magnesia in Thessaly (Greece) where magnetic loadstone (Magnetite, Fe, O) is found as a natural resource [1]. The first reports, in Europe, of the attraction and repulsion forces arising between magnetic loadstones were made by Thales of Miletus around 600 BCE. The expression "sensor" is derived from the Latin "sensus" meaning capable of sensitivity. It is gradually replacing previously used expressions such as "measurement pick-up" and "probe." The directional compass can be regarded as the first magnetic sensor since it reacts to the Earth's magnetic field. Its history stretches back over 4000 years and can be traced to the Chinese who first discovered magnetic loadstone as a natural source of magnetism and used it as a directional aid for orientation [2]. The compass became significantly more important in Europe from about 1200 CE onwards, and in particular, around the time of the great seafaring adventurers and explorers. On his transatlantic voyages, Christopher Columbus observed the behavior of the compass as he sailed westward; famous compass-makers are known to have lived in London and Nurnberg around 1500. In 1820, Oersted discovered that a current-carrying wire deflected a compass needle in its vicinity, and with that the age of electromagnetism had arrived. The first mathematical formula describing the correlation between electric current and magnetism through the deflection of a magnetic needle was Biot–Savart's law. Faraday repeated and extended Oersted's experiments and while doing so discovered the Law of Induction in 1831. The first magnetometer to be constructed was the bifilar magnetometer built in 1831 by Gauss and Weber and the Weber–Bussole compass in 1841, which included a magnetic needle used to measure powerful currents. In 1862, Maxwell created the common theoretical basis for electromagnetism with laws which were named after him, though the expression "permeability" can be traced to Lord Kelvin. Throughout the history of this topic it is evident that the availability of different types of sensors operating on a magnetic basis is very closely linked to the development and availability of special magnetic materials and to the discovery of new physical and magnetic effects. Some of these effects were very soon exploited to make new magnetic sensors, others were not used until much later, and some are yet to be utilized in sensors. Table 1.1 gives a brief history of the use of magnetic effects in sensors, see also [3].

1.3 Natural and Technical Magnetic Fields and Their Order of Magnitude

Both our natural environment and our technical surroundings provide magnetic fields of many different types and orders of magnitude [1]. Many magnetic sensors detect such fields either directly or indirectly using various principles. Hence, it is essential to take a closer look at the types and magnitudes of the various fields.

1.3.1 Natural Magnetic Fields

1.3.1.1 The Earth's Magnetic Field

The most ubiquitous natural field of all is the magnetic field of the Earth which surrounds us perpetually. It is a dipole field, whose field lines originate at the magnetic poles in the interior of the earth, escaping through the surface and reaching into outer space (Figure 1.1). The Earth's magnetic field is used every day by people with compasses to determine the direction or at altitudes of several hundred kilometers to stabilize satellites; on the Earth's surface it can be employed as a constant reference field within certain ranges and times. The precise determination of the parameters of the Earth's magnetic field, namely its magnitude and direction, was one of the great pioneer acts in the field of magnetism and went back to the works of Gauss and Oersted [1].

1.3.1.2 Magnetic Fields in Outer Space

With the aid of satellites and sensitive magnetic-field sensors, magnetic fields in the vicinity of planets and in outer space can also be determined directly, see Table 1.2 and [4].

1.3.1.3 Biomagnetic Fields

Human beings also produce small magnetic fields, which are primarily caused by microcurrents in cardiac, brain, and muscle tissues [5]. They can nowadays

Table 1.1 History in examples: the magnetic effects in first magnetic sensors [1].

Year	Effect	Explanation	Technical use
1842	Joule effect	Change in the shape of ferromagnetic body with magnetization (magnetostriction)	In combination with piezoelectric elements for magnetometers and potentiometers
1846	AE effect	Change in Young's modulus with magnetization	Acoustic delay line components for magnetic field measurement
1847	Matteucci effect	Torsion of a ferromagnetic rod in a longitudinal field changes magnetization	Magnetoelastic sensors
1856	Magnetoresistance (Thomson effect)	Change in resistance with magnetic field	Magnetoresistive sensors
1858	Wiedemann effect	A torsion is produced in a current-carrying ferromagnetic rod when subjected to a longitudinal field	Torque and force measurement
1865	Villari effect	Effect on magnetization by tensile or compressive strength	Magnetoelastic sensors
1879	Hall effect	A current carrying crystal produces a transverse voltage when subjected to a magnetic field vertical to its surface	Magnetogalvanic sensors
1903	Skin effect	Displacement of current from the interior of material to surface layer due to eddy currents	Distance sensors, proximity sensors
1931	Sixtus–Tonks effect	Pulse magnetization by large Barkhausen jumps	Wiegand and pulse-wire sensors
1962	Josephson effect	Tunnel effect between two superconducting materials with an extremely thin separating layer; quantum effect	SQUID magnetometers

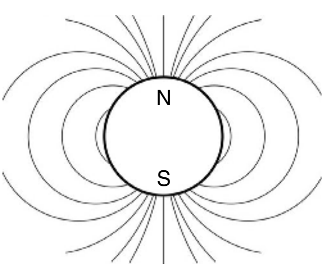

Figure 1.1 Magnetic field formed around the Earth.

Table 1.2 Magnetic field strengths of celestial bodies and objects in outer space [1].

Celestial bodies	Field strength (A/cm)	Flux density (mT)
Galaxies	$\approx 0.15 - 0.25 \times 10^{-6}$	$0.2 - 0.3 \times 10^{-6}$
Mercury (poles)	$\approx 3 \times 10^{-3}$	0.35×10^{-3}
Jupiter (Poles)	Up to 6	Up to 0.8
Mars	0	0
Saturn (equator)	$\approx 2.4 - 16$	$0.3 - 2$
Sun (surface)	$\approx 4 - 8$	$0.5 - 1$
Earth (poles)	≈ 0.5	0.06
A-stars	Up to 28×10^3 A/cm	Up to 3.5 T

be measured with highly sensitive magnetic-field detectors such as flux-gate magnetometers, superconducting quantum interference devices (SQUIDs), and gradiometer coils on the surface of the body, whereas in the past, it had only been possible to measure these currents indirectly by attaching electrodes to the skin and measuring the relevant voltage drops, a technique which forms the basis for the electrocardiogram (ECG). The magnitude of the field strengths and flux densities produced by the heart and brain currents are approximately 50×10^{-3} nT and 1×10^{-3} nT, respectively [6].

1.3.2 Technical Magnetic Fields

1.3.2.1 Magnetic Fields in the Vicinity of Transformers and Electric Motors

Magnetic fields produced in electrotechnical devices, equipment, and plants are usually in the field-strength range of $0.1–10^4$ A/cm [1]. In most cases, these would be AC fields emitted by overhead lines, electrified lines (train or tram lines, etc.), transformers, and electrically powered machinery. Transformers and machinery are mostly operated near the saturation limit of their iron cores, and as such the polarization in the core material attains a level of about 2 T. Similarly, both flux densities in the air gaps of big choke coils or in the gaps between rotors and stators of electric machinery and the stray fields in the vicinity are, as a rule, not much lower.

1.3.2.2 Fields of Permanent Magnets

Except for electromagnets, permanent magnets and magnetic systems are frequently used to produce static magnetic fields, particularly in measurement devices. In such cases, the field is mostly concentrated into a specified volume (e.g. operating air gap) through appropriate design of the magnet and magnetic circuit. The magnitude of the field strengths or flux densities attainable depends on both the remanence and the energy density of the magnetic materials as well as on the geometry of the magnetic circuit. Solenoids with a conventional design, iron-cored coils (electromagnets), and superconducting (solenoid) coils can produce flux densities in the region of 1–100 T depending on their dimensions, their magnitude, and their mode of operation [7–9]. Superconducting coils in medical scanning machines (NMR systems) with a practical diameter of roughly 1 m can produce fields of 1 –2 T, and individual coils with large diameters are used for specified tasks in elementary particle physics and nuclear fusion producing flux densities anywhere from 2 to 10 T.

1.4 Magnetic Terms and Units

The subject of magnetism generates a number of terms and units which are commonly used, the more important ones being included in Table 1.3 [1]. Nowadays, magnetic terms and units are given using the MKSA system, a subsystem of the SI system, and they are based on the four basic units of meter, kilogram, second, and ampere. Although the previously used electromagnetic system of dimensions (CGS electromagnetic units, emu), also known as the Gauss system, is officially no longer acceptable, it is still sometimes found in

Table 1.3 Magnetic terms and units [1].

Term	Quantity	MKSA unit	Subunits	CGS unit	Conversion
Magnetic field strength	H	A/m	1 A/cm = 100 A/m	Oe (Oersted)	1 Oe = 79.58 A/m
Magnetization	M	A/m	See field strength		
Magnetic induction	B	T	1 mT = 10^{-3} T	G (Gauss)	1 G = 10^{-4} T
Magnetic flux	ϕ	Wb	—	Mx (Maxwell)	1 Mx = 10^{-8} Wb
Magnetic polarization	J	T	See induction		
Permeability (absolute)	P	T·m/A	—	G/Oe	
Permeability of vacuum (magnetic constant)	μ_0	$4 \times \pi 10^{-7}$ T·m/A	$0.4 \times \pi 10^{-7}$ T·m/A	1	—

the literature and so a conversion table (Table 1.3) for the CGS units has been included [10].

The most important basic equations are:

$$B = \mu_0 \cdot (H + M) = \mu_0 \cdot H + J \tag{1.1}$$

$$M = \frac{B}{\mu_0} - H \tag{1.2}$$

$$\mu = \mu_0 \cdot \mu_r \qquad \mu_r = \text{Relative permeability} \tag{1.3}$$

$$B = \mu_0 \cdot \mu_r \cdot H \tag{1.4}$$

where, B is magnetic induction, μ_0 is permeability of vacuum, H is magnetic field strength, J is magnetic polarization.

1.5 Magnetic (Micro) Sensors

1.5.1 Definition of Magnetic Sensors

Magnetic materials, i.e. soft and hard magnetic materials and all other materials, which are sensitive to magnetic fields, play a principal role in the nature and operation of magnetic sensors. But at this stage it is not relevant to consider whether metals, metal oxides, or semiconductors are concerned, or which magnetic field is influencing physical properties [11–14]. In textbooks on measurements and control, books on sensors and review articles, sensors have been classified using the following methods [15, 16]: Types of sensors; Physical principles; Properties measured; Sensor applications; Sensor technologies. For example, in [1], a classification system has been selected which is primarily based on physical principles and effects, as follows: Magnetogalvanic sensors; Magnetoelastic sensors; Magnetic-field sensors: saturation-core magnetometers (flux-gate magnetometers) and induction-coil and search-coil magnetometers; Inductive sensors (including eddy-current sensors); Wiegand and pulse-wire sensors; Magnetoresistive sensors; SQUID sensors. Microsensors for a magnetic field are modulating transducers (all semiconductor sensors and all silicon sensors) [17]. They convert the magnetic field, whether it is constant or variable, or even of biological origin, if possible, with a maximal degree of accuracy and reliability, into an output electrical signal (current, voltage, or frequency) with high fidelity. The output energy of the modulating sensors is fed by an external power source through an additional input. More specifically, these microdevices are fabricated using standard semiconductor IC technologies (most frequently, silicon processing technologies). Contemporary microsystems for magnetic fields (hybrid or monolithic) must integrate at least two functions. One of them must be the sensing by an input transducer or sensor of the strength and the direction of this physical measurand; the other can be signal processing (when necessary, including a processor and the corresponding software) and/or an actuator. Elements that locally enhance, compensate, or change the direction of the external magnetic field such as ferrite flux concentrators or coils, can also be installed in the microsystem [1, 18–20]. By using appropriate packages with small dimensions, these MEMS offer a variety of contactless sensing.

1.5.2 Soft and Hard Magnetic Materials for Sensors

Almost all magnetic sensors include magnetic materials in the form of active or passive components, and to a large extent, they determine the concept, construction, and ultimately the sensitivity of the sensors. In view of this, a brief survey of magnetic materials and their most important characteristic is presented in Tables 1.4 and 1.5. These materials are classified according to the IEC system for soft and hard magnetic materials. For textbooks on materials refer to [21, 24]. The magnetic materials listed in Tables 1.4 and 1.5 are closely related to the main classes of magnetic sensors shown in Table 1.6 although some special materials have been added.

1.5.2.1 Shape of the Hysteresis Loop

The most typical characteristic of soft magnetic materials is its hysteresis loop. The shape of the loop can vary greatly and is determined by the type of material and its structure which can be changed by processing and annealing. This is

Table 1.4 Soft magnetic materials [1].

Group	Code	
	A	Irons
	B	Low carbon mild steel
	C	Silicon steel, mainly with 3% Si
Crystal metals	D	Other steels
	E	Nickel–iron alloys (five groups E1 – E5 with 30% – 83% Ni)
	F	Iron–cobalt alloys (three groups F1 – F3 with 23% – 50% Co)
	G	Other alloys as AlSiFe-alloys
Oxides	H	Soft ferrites as NiZn and MnZn oxides
Amorphous metal	I	Amorphous alloys (Fe-based and Co-based alloys)
Powder composite metals	—	Based on Fe and iron alloy powders

Table 1.5 Hard magnetic materials [21–23].

Group	Code	
Crystal metals	R1	Alloys of AlNiCo-type
	R2	Platinum–cobalt alloys
	R3	Iron–cobalt–vanadium (Chromium) alloys
	R6	Chromium–iron–cobalt alloys
	R5	Rare earth cobalt alloys
	R7	Rare earth iron alloys
Amorphous metal	—	Rare earth iron alloys
Oxides	Sl	Hard ferrites as Ba- and Sr-ferrites
	T	Other hard magnetic materials, e.g. magnetically semi hard metals

Table 1.6 Magnetic material for sensors (materials are defined in Tables 1.4 and 1.5).

	Magnetically soft		Magnetically hard	
Sensor class	**Material**	**Useful for**	**Material**	**Useful for**
Magnetogalvanic	C, E	Slotted cores yokes	R1, R5, R7	Magnetic circuit
Magnetoelastic	D, E1, I, C, E1	Shafts, surface layers for shafts, laminated core packages, pot-cores	—	—
Fluxgate	E1, H, I	Strips and rods, toroidal cores	—	—
Inductive, eddy current	C, E2, E3, H	Rods, yokes, laminated cores, pot core, rods	R1, R5, R7, S1	Parts
Wiegand, pulse-wire	F, special alloys	Wires	R6	Magnets as rods for switching
Magnetoresistive	E1, I, NiCo, NiFeCo	Resistors	R2, R5, CoCr	Permagnetizing layers

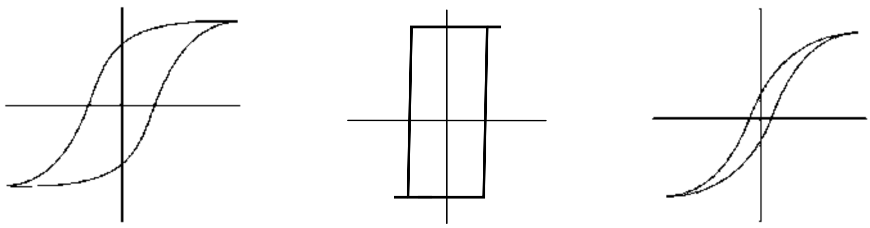

Figure 1.2 Three main types of the shapes of hysteresis loops in different materials. *Source:* adapted from [1].

valid for both metals and oxides. The three main types of loop are shown in Figure 1.2 [25].

As the number of magnetic materials currently available is vast, there seems little point in providing extensive tables of material data. This information is published in standard monographs and company catalogues. Instead, we have chosen to present the ranges of variation of the most critical magnetic material terms found in survey diagrams.

1.5.2.2 Saturation Polarization J_s and Coercivity H_c

Two of the most essential material terms are saturation polarization J_s, which gives an idea of the amount of material required for a particular component and coercivity H_c, which provides the basis for classification of the magnetic material concerning its hard and soft magnetic qualities. Figure 1.3 shows a plot of saturation polarization J_s versus the coercivity H_c, where J_s is plotted on a linear scale and H_c on a logarithmic scale, since the materials currently available range from extremely soft alloys, such as permalloy, to commercial iron and steel, covering approximately four to five orders of magnitude.

1.5.2.3 Initial Permeability μ_i

Another critical property of soft magnetic materials is the (relative) initial permeability μ_i. Crystalline 72–83% NiFe alloys and cobalt-based amorphous alloys have the highest initial permeability, with a value of more than 100 000. Mid-range permeabilities in the region of 2000–15 000 occur in NiFe alloys with 36–50% Ni and also in ferrites. Low initial permeability values of 300–1500 are typical for iron, silicon–iron, cobalt–iron, and some ferrites. Even lower values, in the region of 50–300, occur with powder composite materials and ferrites and very low permeabilities (down to values of 5–10) are typical for some special powder composite materials and special ferrites.

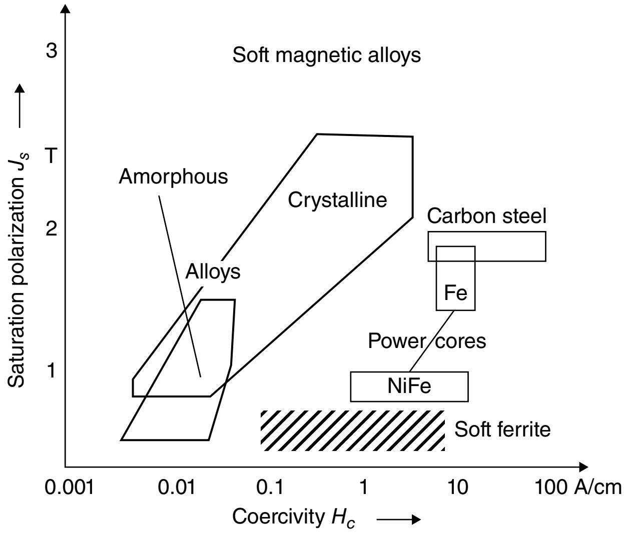

Figure 1.3 Survey on soft magnetic materials plot of saturation polarisation J_s versus the coercivity H_c, where J_s is plotted on a linear scale and H_c on a logarithmic scale. *Source:* adapted from [1].

1.5.2.4 Specific Electrical Resistivity ρ

The difference between the specific electrical resistivity of metals and that of ferrites is several orders of magnitude, as a result of which, for AC-field applications, metals require laminated cores whereas ferrites and powder composites can be used directly as compact cores and parts. Figure 1.4 shows the range of the specific electrical resistivity ρ for metals, ferrites, and powder composites.

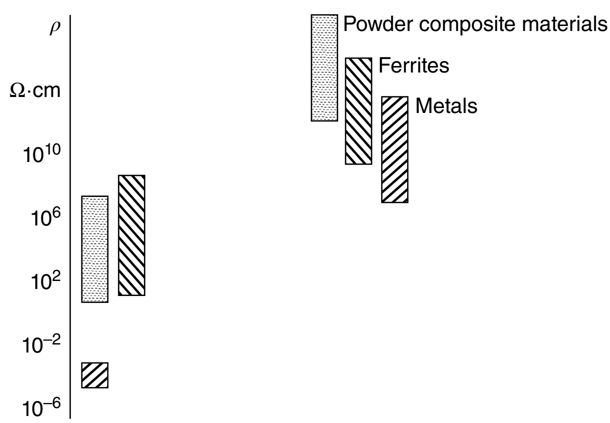

Figure 1.4 Specific electrical resistivity of magnetic materials. *Source:* adapted from [1].

1.5.3 Mechanical Properties of Magnetic Materials

In certain sensor types, the mechanical properties of materials are also important, for example, in magnetoelastic sensors the hardness, yield strength, compressive strength, Young's modulus, etc. must all be considered. Several of the mechanical properties of soft and hard magnetic materials have been compiled in Table 1.7.

1.5.4 Relations Between Sensing Techniques and Sensor Applications

Two categories of applications of magnetic sensors and microsystems can be distinguished: direct and indirect [1, 17, 18, 20, 26]. Direct registrations are those in which only information about the magnetic field (strength and

Table 1.7 Mechanical properties of magnetic materials [1].

Material group		Vickers hardness (HV)	Yield strength (N/mm^2)	Young's modulus (kN/mm^2)
Magnetically soft	Metals Crystalline	80 – 200	150 – 500	100 – 230
	Metals amorphous	800 – 1000	1500 – 2000	~150
			Compressive strength (N/mm^2)	
	Soft ferrites	800	75 – 100	150
Magnetically hard	Powder composite metals	—	60 – 250	~50
			Yield strength (N/mm^2)	
	Malleable alloys like FeCoCr, FeCoV	450 – 950	1000 – 1500	245 – 255
			Compressive strength (N/mm^2)	
	Metals, cat AlNiCo, magnets	400 – 700	120	—
	RE magnets (SmCo, NdFeB)	550 – 650	850 – 1000	110 – 150
	Hard ferrites	600 – 1000	500 – 800	150

direction) itself is required. Indirect sensor systems use the field as an intermediary carrier to measure a nonmagnetic quantity (tandem transducers). Examples of direct applications include the following:

- Readout of information stored on disk, tape, and bubble memory
- Recognition of magnetic patterns on banknotes and credit cards
- Magnetometry: control of a magnetic apparatus such as classical and superconducting electromagnets; instrumentation for particle accelerators as well as the determination of the full magnetic field vector, its direction, and its gradient by detecting two or all three vector components
- Magnetic levitation control
- Earth magnetic-field measurement and the electronic compass
- Geomagnetic remote sensing for geological and volcanic surveying
- Attitude control for satellites
- Positioning of aircrafts, ships, missiles, projectiles, or submarines by the perturbations they cause in the geomagnetic field, and for the development of global navigation systems
- Biomagnetometry: obtaining diagnostic data by cardiomagnetism, myomagnetism, and neuromagnetism to map the functions of the heart, muscles, nerves, and brains of humans and animals

Indirect applications are much more common [1, 17, 18, 20, 26–30]. Examples include the following:

- Distance (linear and angular), velocity, speed, and vibration measurements
- Position detection
- Rotation and direction of rotation, e.g. for tachometry
- Collector-less DC motor control
- Keyboards and proximity switches
- Microphones
- Angular displacement detection and angle decoders and synchro resolvers
- Linear and rotary potentiometers, and crankshaft position transducers in automobile ignition control
- Automotive antiskid breaking systems
- Nondestructive magnetic methods, including characterization of materials and metal detection
- Electrical current and power measurements (watt-hour meters) that do not interrupt the current-carrying conductor
- Analog multiplication
- Galvanic isolation
- Traffic detection when a ferromagnetic body is passing
- Measurement of mechanical and chemical parameters, pressure, mass filters, and so on, using suitable magneto-modulating systems that contain permanent magnets.

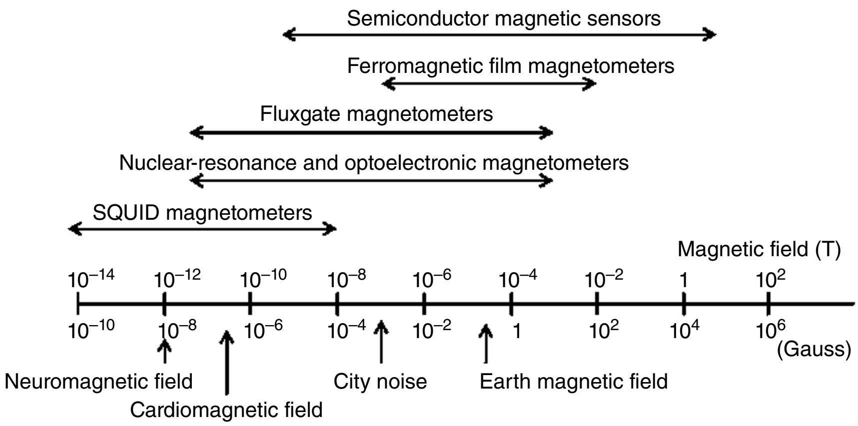

Figure 1.5 Field range of five principally different types of magnetic transducers and microsystems. *Source:* adapted from [17].

These incomplete lists of the magnetic sensor and microsystem applications should suffice to show how universal they are. From the viewpoint of the achieved accuracy, these are some of the most precise instruments available in control-measurement technology. The range of operation of various magnetic sensors and microsystems is systematized in Figure 1.5. The applications selected above clearly show the wide variety of fields met by magnetic (micro) sensors. It ranges from the biosignals, which are lower than 10 fT; passing through the variations of the geomagnetic field (~0.05 mT) through the most important large-scale applications, using permanent magnets with induction fields at about 50 mT. With the recording of magnetic fields ranging from 0.01 to 10 mT, reach to flux densities of several Tesla in the apparatus for nuclear physics and the colossal inductions of millions of Tesla in the new stars and black holes of the universe. Therefore, there is a dynamic range of fields not less than 15–16 orders of magnitude! As seen from Figure 1.5, at least five principally different types of devices are capable of measuring this unique range of magnetic fields: superconductor magnetic sensors such as SQUIDs, nuclear-resonance and optoelectronic magnetic transducers, flux gate magnetometers, ferromagnetic thin-film magnetoresistors, and semiconductor magnetic devices. That is why this broad range cannot be covered by only one type of magnetic sensor microsystem.

1.5.5 Classification of Magnetic Sensors

The great variety of applications, the peculiarities of transducer action and reliability, the growing research activity and the necessity to compare the results, the demanding requirements concerning the quality of used materials, and the

Table 1.8 Classification of the principal figures of merit of magnetic sensors [17].

$OUT(B)_{C=const}$	$OUT(C)_{B=const}$	System descriptors
Sensitivity	Noise	Excitation
Nonlinearity	Offset	Input impedance
Calibration	Cross-sensitivity	Output impedance
Range	Drift	Size
Frequency response	Creep	Weight
Directivity	Temperature error	Packaging
Resolution	Operating life	Sensor material
Accuracy	Reliability	Environmental condition
Hysteresis	Long-term stability	Device design
Error (reversibility error)	Response time	
Output form		

tendency for unification necessitate the development of clear criteria for evaluation of the different sensors, including the magnetic sensor microsystems. Consideration of all figures of merit can be made more comprehensible if magnetic sensors are classified into three groups [20], as follows:

1) The change of the output (*OUT*) in a magnetic field *B*, keeping (or leaving) constant other possible external influences, e.g. temperature *T*, pressure *P*, and radiation *Φ*, summarized here with the symbol *C*. The denotation of these characteristics is $OUT(B)_C$.
2) The behavior of the output signal *OUT* as a function of all possible external influences *C* at a constant (or absent) magnetic field *B*, denoted $OUT(C)_B$.
3) The parameters describing the magnetic sensor as a device, denoted SD (system descriptors).

In Table 1.8, the principal figures of merit of magnetic-field microsensors are presented according to this classification.

1.6 Characteristics of Magnetic Sensors

1.6.1 Characteristics Related to $OUT(B)_C$

1.6.1.1 Magnetosensitivity

By definition, the sensitivity *S* or the transduction efficiency is the ratio of the change of the output signal (current, voltage, or frequency) to the variation of the external magnetic field *B* at a constant *T*, *P*, *Φ*, etc. Both an absolute sensitivity and a relative sensitivity of the modulating magnetosensors can be defined [1, 20, 27, 31]. Equations (1.5)–(1.7) define the absolute sensitivity when the output is a current I, voltage V, or frequency f, respectively:

$$S_A^{(V)} = \left|\frac{\partial V}{\partial B}\right|_C, \left[\mathrm{VT}^{-1}\right] \tag{1.5}$$

$$S_A^{(I)} = \left|\frac{\partial I}{\partial B}\right|_C, \left[\mathrm{AT}^{-1}\right] \tag{1.6}$$

$$S_A^{(f)} = \left|\frac{\partial f}{\partial B}\right|_C, \left[\mathrm{HzT}^{-1}\right] \tag{1.7}$$

The relative magnetosensitivity is determined by the ratio of the absolute sensitivity to the supply current or voltage applied to the additional transducer input. The figure of merit is the current-related sensitivity S_{RI} (Eq. 1.8) when a supply current I_S feeds the additional input, and the voltage-related sensitivity S_{RV} (Eq. 1.9) when a supply voltage V_S feeds the additional input:

$$S_{RI}^{(V)} = \frac{S_A^{(V)}}{I_S} = \left|\frac{1}{I_S}\frac{\partial V}{\partial B}\right|_C, \left[\mathrm{VA}^{-1}\mathrm{T}^{-1}\right]$$

$$S_{RI}^{(I)} = \frac{S_A^{(I)}}{I_S} = \left|\frac{1}{I_S}\frac{\partial I}{\partial B}\right|_C, \left[\mathrm{T}^{-1}\right]$$

$$S_{RI}^{(f)} = \frac{S_A^{(f)}}{I_S} = \left|\frac{1}{I_S}\frac{\partial f}{\partial B}\right|_C, \left[\mathrm{HzA}^{-1}\mathrm{T}^{-1}\right] \tag{1.8}$$

$$S_{RV}^{(V)} = \frac{S_A^{(V)}}{I_S} = \left|\frac{1}{V_S}\frac{\partial V}{\partial B}\right|_C, \left[\mathrm{T}^{-1}\right]$$

$$S_{RV}^{(I)} = \frac{S_A^{(I)}}{V_S} = \left|\frac{1}{V_S}\frac{\partial I}{\partial B}\right|_C, \left[\mathrm{AV}^{-1}\mathrm{T}^{-1}\right]$$

$$S_{RV}^{(f)} = \frac{S_A^{(f)}}{V_S} = \left|\frac{1}{V_S}\frac{\partial f}{\partial B}\right|_C, \left[\mathrm{HzV}^{-1}\mathrm{T}^{-1}\right] \tag{1.9}$$

The relative sensitivity should be suitable to the comparative analysis of magnetic microdevices, while in the purely practical applications, the absolute sensitivity is preferred.

1.6.1.2 Nonlinearity

When the ideal output characteristic of the magnetosensor is a straight line, the deviation of the real output characteristic from it is a relative error that is termed a nonlinearity (NL). This parameter is determined by the expression

$$NL \equiv \frac{|OUT_1 - OUT_2|}{(OUT_2)} 100\% \tag{1.10}$$

where OUT_1 is the measured value of the output signal at a given fixed magnetic induction B_o, and OUT_2 is the corresponding value from the straight line at a field B_o. This line is the best fit to the measured output values.

1.6.1.3 Calibration

This figure of merit is necessary to determine the real output signal $OUT(B)$ of any magnetosensor. The calibration is a test during which known values of the magnetic induction (taking into account the sign of B) are applied to the microtransducer and the corresponding output readings are recorded [20, 31].

1.6.1.4 Sensor Excitation

An important feature of the magnetosensitive device is the manner of their excitation by the field B, i.e. whether the vector B is perpendicular or parallel to the active surface of the structure [20, 31]. Depending on the orientation of B with respect to the plane of the device, we have divided the magnetic microsensors known so far into orthogonal and parallel-field transducers.

1.6.1.5 Frequency Response

The dynamic behavior of the magnetic field sensors is of primary importance in the measurement of fast variations of the field B. The frequency response is the dependence of the amplitude ratio of the output signal to the AC field B on the frequency of the external sine wave of the AC field B within a specified frequency interval. It is generally accepted that the dynamic degradation of a microtransducer in an AC field B starts with a reduction of the output by a factor $1/2$, i.e. by 3 db [20, 31].

1.6.1.6 Resolution

This characteristic determines the smallest possible step change of the magnetic induction, which can be detected on the sensor output [20, 31].

1.6.1.7 Error

This figure of merit is the algebraic difference between the magnetic field recorded at the sensor output and its exact value. The error is expressed as a percentage of the full-scale output. The error curve is a graphical representation of the errors obtained from a certain number of calibration cycles. There is a slight error given in percent termed reversibility error. It expresses the difference in the output readings of the magnetotransducer at fixed value B_o with changes in the magnetic-field B direction (from positive to negative and vice versa). This error strongly depends on the difference in the contact area and nonuniformity of the sensor material used [18, 20, 31].

1.6.1.8 Accuracy

This characteristic is defined as a ratio of the error to the full output scale expressed as a percentage. The accuracy can be presented in the same units by which the magnetic field is measured as within ± … % of the full scale output [18, 20, 31].

1.6.1.9 Hysteresis

This parameter determines the maximal change in the output signals for any fixed value B_o of the magnetic induction within the specified range. The value B_o is reached first by increasing and then by decreasing the external field B. The hysteresis is expressed as a percentage of the full-scale output during any calibration cycle [18, 20, 31].

1.6.1.10 Repeatability

The ability of a magnetic microsensor to give the same output when the same measurand value B_o is applied. It is expressed as a percentage of the full-scale output. Many calibration cycles are needed to determine the repeatability [18, 20, 31].

1.6.2 Characteristics Related to $OUT(C)_B$

1.6.2.1 Noise

The output electrical noise is a fundamental property that determines the lowest detected value of the magnetic field B_{min}[1, 18–20, 27, 31]. In this output signal (voltage or current) with a random amplitude and random frequency, which has nothing in common with the measurand B, the most disturbing component is $1/f$ noise. By selection of a more qualitative semiconductor material and more sophisticated technological steps, the $1/f$ noise can be significantly reduced. Often this figure of merit is presented as an equivalent magnetic-field noise at a signal-to-noise ratio equal to one.

1.6.2.2 Offset

The offset is a parasitic output signal in magnetic microsensors of a modulating type (in most cases with a differential output) in the absence of a magnetic field B. Without any supplementary information about the value of induction B, the offset cannot be distinguished from the useful output signal (voltage, current, or frequency):

$$OUT(B) = SB + OUT'(B = 0) \tag{1.11}$$

where $OUT'(B = 0)$ is the offset that is most frequently the result of a structural or electrical asymmetry of the sensor. This error is often expressed as within + … % of the full-scale output [1, 18–20, 27, 31]. A more relevant definition of the offset is its expression as a signal of an ideal sensor (without offset) generated by an equivalent magnetic induction $B_{off,\ eq} \equiv B_{off}$:

$$B_{off,eq} \equiv \frac{V_{off}}{S_A^{(V)}}; \quad B_{off,eq} \equiv \frac{I_{off}}{S_A^{(I)}}; \quad B_{off,eq} \equiv \frac{f_{off}}{S_A^{(f)}} \tag{1.12}$$

1.6.2.3 Cross-Sensitivity and Temperature Error

The influence of one or more measurands as pressure P, light Φ, temperature T, and so forth, on the magnetosensitivity is an undesired parasitic output signal termed cross-sensitivity (CS) [1, 18–20, 27, 31]. The figure-of-merit CS is expressed as $CS \equiv (1/S\ \partial S/\partial C)$, where S is the sensor magnetosensitivity (Eqs. 1.5–1.9) and C is the source of perturbation. Most frequently this is the temperature T; consequently,

$$TC \equiv \left(\frac{1}{S}\right)\left(\frac{\partial S}{\partial T}\right)100\% \tag{1.13}$$

In this case, TC is the temperature coefficient of magnetosensitivity, measured as % K^{-1} or % C^{-1}. The temperature interval (T_{min}, T_{max}) within which the value of the TC is constant should be specified.

1.6.2.4 Drift and Creep

The drift is an undesirable slow change in time of the output signal at a constant magnetic field B. The drift is in no way connected with the measurand B. Drift can be caused by temperature, pressure, light, and so on. The creep, which is also a parasitic magnetosensor fluctuation, is a weak and continuous change at the output at constant magnetic field B and all other environmental parameters such as T, P, and Φ [20, 31].

1.6.2.5 Response Time

This figure of merit determines the time it takes for the sensor output signal to reach its final value as a result of a step change of the magnetic field. This parameter is indicated in the handbooks, for example, as "95% response time … μ_s" [18, 20, 31].

1.6.3 Characteristics Related to the System Description

1.6.3.1 Electrical Excitation

This is the external electrical voltage and/or current applied to a magnetic modulating microsensor for its proper operation.

1.6.3.2 Input and Output Impedance

The input impedance presented to the power supply is measured between the excitation terminals. The output impedance is measured between the output leads of the magnetic sensor under conditions with open-circuited additional input terminals.

1.6.3.3 Environmental Conditions

Magnetic-field microsensors most frequently function under the following environmental conditions: temperature (25 ± 10) °C or (77 ± 18) °F, relative humidity 90% or less, and barometric pressure 26–32 inches Hg. The remaining figures of merit of the magnetic devices, as well as other characteristics, methods, and circuits for their determination, can be found in the literature [18, 20, 31] and the references therein.

1.7 Magnetic Noise

Any macroscopic quantity in a system such as voltage, current, or resistance is subject to fluctuations around its mean value. These fluctuations are created by the random contributions to the transport or by internal displacements of atoms [32]. The first point of view is to consider that these fluctuations are strongly related to the properties of the material and their study gives a new approach to understand processes in condensed matter. A second point of view more related to applications is to call these fluctuations noise which is related to the quality of the material investigated. Reduction of this noise becomes a target for magnetic sensor applications.

1.7.1 Noise Formalism

In this part, we give some bases necessary for the analysis of noise measurements in GMRs with a highlight on some common traps in noise treatment. We will not address here extensively the quantum approach of fluctuations as magnetoresistive sensors have size and working temperature, which can be handled with a classical treatment.

1.7.1.1 Fluctuations, Average and Distribution

We consider a fluctuating quantity $V(t)$. The voltage V is the most common quantity measured in magnetic sensors, but the following treatment can be applied to any relevant quantity like the current, the resistance, or the charge. In an experiment, $V(t)$ is often measured at discrete times $t_1, \ldots, t_n$ by some acquisition system but it can also be treated in an analog way with some integration, derivation, analog multiplication, or other mathematical operation.

Any nonlinear operation has to be carefully handled in order to avoid spurious deformation of the signals. Then a number of new quantities can be derived from that measurement. The first one is the average

$$\bar{V} = \frac{1}{n}\sum_{i=1}^{n} V(t_i) \tag{1.14}$$

A formal definition of the average, easier to manipulate is:

$$\bar{V} = \lim_{T\to\infty} \frac{1}{T}\int_0^T V(t)dt \tag{1.15}$$

where T is the duration of the measurement. In the following, we use the second formalism. It should be noticed that this average is also a fluctuating quantity on a time scale T corresponding to the total acquisition time. In common systems, if T is long enough this average is representative of V but in some cases like in presence of slow magnetic relaxation, $\bar{V}$ can be very dependent of the history of the system. The second quantity is the variance of V. It is defined as

$$\sigma^2 = \frac{1}{n}\sum_{i=1}^{n} (V(t_i) - \bar{V})^2$$

or

$$\sigma^2 = \lim_{T\to\infty} \frac{1}{T}\int_0^T (V(t_i) - \bar{V})^2 dt \tag{1.16}$$

It measures the exploration in amplitude of V. σ is an easy comparison of different signals but sometimes a spurious frequency may appear in the signal like the line frequency (50 or 60 Hz) which dominates and sets the value of σ. For large systems, the knowledge of σ and $\bar{V}$ is sufficient to know the distribution function ρ of V. This is due to a very useful theorem, the central limit theorem, which demonstrates that a sum of n random identical quantities tends very rapidly to a normal (or Gaussian) distribution law when n grows.

$$\rho(V) = \frac{1}{\sqrt{2\pi\sigma^2}}\exp\left(\frac{(V-\bar{V})^2}{2\sigma^2}\right) \tag{1.17}$$

For example, the voltage across an MR with a fixed sensing current can be divided in smaller identical MRs which individually fluctuates and hence one can easily demonstrate that the distribution of the voltage follows a normal distribution. Another very common fluctuation is the random jump between two discrete levels. This type of fluctuation is, for example, the Random Telegraph Noise (RTN) described later. The jumps are arising from a level 1 to a level 2 with a w_1 probability to stay at level 1 and w_2 probability to stay at level 2.

The mean period of these jumps is τ. The distribution is then showing peaks centered on the values of the levels with a width related to the additional noise. Hence, analysis of the distribution may help to distinguish the presence of discrete levels.

1.7.1.2 Correlations

In time domain, correlations are very important because they give a measure of the similarities between two functions (cross-correlations) or for the same function but at two different times (autocorrelation). The autocorrelation is a measure of the memory of the system. The general form of the correlation of two functions X and Y is defined as the average of the functions at a time difference of τ.

$$C_{xy}(\tau) = \lim_{T\to\infty} \frac{1}{T}\frac{1}{2\pi}\int_0^T X(t)Y^*(t-\tau)dt \tag{1.18}$$

The autocorrelation function is then

$$g_x(\tau) = \lim_{T\to\infty} \frac{1}{T}\frac{1}{2\pi}\int_0^T X(t)Y^*(t-\tau)dt \tag{1.19}$$

The autocorrelation at $\tau = 0$ is simply the mean square value of the fluctuations. For example, a thermal noise has an autocorrelation function which is zero except for $\tau = 0$. This is the signature of a totally random process. However, if you measure a thermal noise through a filter, you may find a nonzero autocorrelation due to the memory injected by the filtering.

It should be noticed that the experimental correlations are dependent on the initial time chosen for the acquisition. Hence, there is a strong hypothesis behind, usually fulfilled by GMR and TMR systems, the stationarity of the system which assumes that the system is at equilibrium and these quantities are independent on the initial measurement time.

1.7.1.3 Frequency Space and Spectral Density

Amplitude and amplitude distribution of fluctuations are analyzed by the tools described previously but spectral analysis gives the frequency dependence of the noise which is essential for separating and understanding the noise sources. The way to switch from time domain to frequency domain is the Fourier transform.

$$V(\omega) = \frac{1}{2\pi}\int_{-\infty}^{\infty} V(t)e^{i\omega t}dt \tag{1.20}$$

We also introduce a more experimental Fourier transform which considers that $V(t)$ is zero outside of the measuring time.

$$V_T(\omega) = \frac{1}{2\pi}\int_{-\infty}^{\infty} V(t)e^{i\omega t}dt \tag{1.21}$$

This well-known form of Fourier transform is however a source of lot of errors in experiments. Firstly, if the total acquisition time is T, the lowest achievable frequency is $2\pi/T$ and the highest is given by $2\pi/t_{acq}$ where t_{acq} is the acquisition time interval. Secondly, if signals are present in the fluctuations at higher frequencies, they will appear by folding in the frequency range. This is the reason why low pass filtering is necessary for noise measurements. Thirdly, Fast Fourier Transform (FFT) algorithms are generally used due to the gain in time of data treatment. As the data are finite in time, a window function is applied on the data. The simplest one is just a rectangular window. The data are then considered as 0 outside the window and multiplied by 1 in the window. However, the jump at the edges created spurious oscillations in the Fourier transform. More sophisticated windows are hence used. The most common are Hann, Hamming, and Gaussian windows. The Hann function consists of multiplying the data by a cosine function, which vanishes for the first and last points. So the quantity calculated becomes:

$$V_{Hann}(\omega) = \frac{1}{2\pi}\int_0^T V(t)e^{i\omega t}\left(1-\left|\cos\left(\frac{\pi t}{T}\right)\right|\right)dt \tag{1.22}$$

Or in the case of Gaussian window,

$$V_{Gauss}(\omega) = \frac{1}{2\pi}\int_0^T V(t)e^{i\omega t}e^{-\frac{(t-(T/2))^2}{2(\sigma T/2)^2}}dt \tag{1.23}$$

On rather flat signals like noise, the windowing has no impact but in case of a strong line signal, it allows suppressing artefacts. The total energy of the signal is given by

$$E = \int_0^T |V(t)|^2 dt \tag{1.24}$$

which can be expressed through the Parseval theorem by

$$E = 2\pi\int_{-\infty}^{\infty} |V(\omega)|^2 d\omega \tag{1.25}$$

Hence the average power associated to the fluctuations can be defined by:

$$P = \lim_{T\to\infty}\frac{1}{T}\int_0^T |V(t)|^2 dt = \lim_{T\to\infty} 2\pi\int_{-\infty}^{\infty}\frac{|V(\omega)|^2}{T}d\omega \tag{1.26}$$

This allows us to define the power spectral density (PSD) as:

$$S_V(\omega) = \lim_{T\to\infty} 2\pi\frac{|V(\omega)|^2}{T} \tag{1.27}$$

The PSD is given for voltage fluctuations in V^2/Hz. A very important point is the relation between the PSD and the autocorrelation function which is the Wiener–Khintchine theorem:

$$S_V(\omega) = 2\int_0^\infty g(\tau)\cos(\tau\omega)|V(\omega)|^2 d\tau \tag{1.28}$$

A major example is an exponentially decreasing autocorrelation function. It is the case for a relaxation process but also for the current in a simple R–L circuit. The autocorrelation decreases with a characteristic time τ_C and is written as:

$$g(\tau) = g(0)\exp\left(-\frac{\tau}{\tau_C}\right) \tag{1.29}$$

The corresponding PSD is

$$S_V(\omega) = 4g(0)\frac{\tau_C}{1+\omega^2\ \tau_C^2} \tag{1.30}$$

This spectrum called Debye–Lorentzian spectrum presents a flat response at low frequencies and a $1/f^2$ decrease at high frequencies with a corner at $1/\tau_C$. This exponential decrease of the autocorrelation function is also valid for RTN noise and hence the RTN signature in the PSD is this Debye–Lorentzian spectrum. Another important remark is related to very slow decrease of the DC level in noise measurements determining the formal spectral density from a noise mechanism. Very often noise measurements setups present a very low frequency high pass filter (0.1 Hz or lower) to avoid amplifier saturation by DC offsets. If there is an external perturbation like a short pulse on the DC line or a jump in the DC signal, this induces a decrease of the output signal with a very long characteristic time and hence a Debye–Lorentzian spectrum with a corner frequency below the measurement range. For that reason, in case of measurement of a $1/f^2$ decrease at very low frequencies, investigation of the DC level fluctuations should be done.

1.7.2 Sensitivity, Signal-to-Noise Ratio, and Detectivity

Noise PSD is given in V^2/Hz but it is usually more convenient to compare a signal given in V to the square root of the PSD which is in $V/\sqrt{Hz}$. In order to evaluate a signal-to-noise ratio, a reference signal at a known frequency generated by a coil is often used. If a signal $V_0\cos(\omega t)$ is seen in the acquisition system, its PSD is the power associated to this signal taken on a bandwidth of 1 Hz so 1 s and it corresponds to $V_0^2/2$. This allows direct calibration of a sensor.

The sensitivity for a magnetoresistive signal, β, is usually given in V/V/T. Typical values for GMR sensors are 20–40 V/V/T or 2–4%/mT.

The output voltage of a magnetoresistive sensor can be written as:

$$V_{out} = ((R_0) + \delta R(H))I \quad (1.31)$$

If the sensor is linearized and well centered, the output can be written as:

$$V_{out} = \left(R_0 + \frac{\delta R}{\delta H} \cdot H + \ldots\right) I \quad (1.32)$$

where the terms with higher H power are small $\delta R/\delta H$ is given in Ohms/Tesla. The sensitivity is given by $(\delta R/\delta H)/R_0$.

In order to compare different sensors, it is very convenient to use the field equivalent noise PSD, sometimes called detectivity. It corresponds to the PSD divided by the sensitivity. For example, if a sensor exhibits a thermal noise of $1\ \mathrm{nV}/\sqrt{\mathrm{Hz}}$ and a sensitivity of 20 V/V/T, the corresponding detectivity will be 50 pT for 1 V of bias voltage.

1.7.3 Different Sources of Noise

1.7.3.1 Separation of Magnetic and Nonmagnetic Noise

It should be noticed that noise in magnetic sensors can or cannot be magnetic-field dependent. A magnetic field-dependent noise appears or disappears with the application of an external field. This is, for example, the case of a part of the $1/f$ noise in magnetoresistive junctions. One way to separate it is to measure the noise of the sensors in the whole range of operation.

1.7.3.2 Frequency-Independent Noise (Thermal or Johnson–Nyquist Noise), Shot Noise

1.7.3.2.1 Thermal Noise

Frequency-independent noise is called white noise and corresponds to processes without any autocorrelation except at zero time. It should be noticed that noise appears flat in the range of measurement because its correlation characteristic time is faster that the minimal sampling time.

The most important noise is the thermal noise, which is directly related to the resistance of the sensor. The first observation of this noise has been done by Johnson [33] and interpreted by Nyquist [34]. The associated PSD is written as:

$$S_V(\omega) = 4RK_BT \quad (1.33)$$

where $K_B = 1.3806 \times 10^{-23}\ \mathrm{J \cdot K^{-1}}$ is the Boltzmann constant. There are several ways to demonstrate this relation, but the base is just to say that the energy available for a dipole of resistance R is $K_BT/2$. This formula is valid for frequencies much lower than $K_BT/\hbar$ where $\hbar$ is the Planck constant. This thermal noise cannot be eliminated or reduced except by changing the resistance or the temperature, but it has the advantage to be independent on the voltage applied on the sensor. It should also be noticed that the impact of this noise on the signal-to-noise ratio is directly related to the working bandwidth. The integrated noise will increase as the square root of the bandwidth.

1.7.3.2.2 Shot Noise

This noise is due to the fact that the electrical current is not continuous due to the discrete nature of the electrons. This noise is detectable only if there is a barrier to cross where the quantum nature of electrons is revealed. In metals, the electrons' inelastic scattering length is very small, typically a few nanometer at room temperature and a metallic sensor could be described as a very large number of individual elements of few nanometer in series and hence the shot noise is divided by the square root of this number [35]. For that reason, shot noise is not present in GMR sensors. In magnetic tunnel junctions, a number of theoretical and experimental works have been recently published. The electrons are following a Poisson law when they pass through a barrier (without quantum or correlation corrections) and hence it is possible to calculate the PSD of the shot noise. At $T = 0$, it is simply given by

$$S_I(\omega) = 2eI \tag{1.34}$$

In mesoscopic systems, deviations of the Poisson statistics are observed and modify Eq. (1.34). A review of noise in mesoscopic systems can be found in [36]. In particular, it has been shown that the statistics can be slightly different from a pure Poisson statistics inducing an enhancement or a reduction of the shot noise [37, 38]. This enhancement or reduction is characterized by the Fano factor F.

1.7.3.2.3 Crossover Between Shot Noise and Thermal Noise

When the temperature is increasing, the shot noise expression must take into account thermal fluctuations. A more general formula should be applied [35]:

$$S_V(\omega) = 2eI\coth\left(\frac{eV}{2K_BT}\right)R^2 \tag{1.35}$$

In the two temperature limits ($T \gg 0$ and $T \to 0$), we find the expression of noise given in Eqs. (1.33) and (1.34), respectively.

1.7.4 Low Frequency Noise

1.7.4.1 1/*f* Noise

$1/f$ noise is a general term referring to a frequency decreasing noise with a power law frequency $1/f^{\beta}$ where β is an exponent typically of the order of 1. This noise is observed in nearly all fluctuating systems including biological and geological fluctuations. In GMR and TMRs, this low frequency noise is dominant and is often a drawback in performances of magnetoresistive sensors. The origin of the $1/f$ noise is resistance fluctuations and not voltage fluctuations like the thermal noise. Hence, these fluctuations can only be revealed by applying a current in the sensor. Voss and Clarke have demonstrated in [39] that the variance of Johnson noise exhibits a $1/f$ power spectrum demonstrating the resistance fluctuation nature of the $1/f$ noise. This resistance fluctuation behavior implies that the PSD is varying as V^2 or I^2. This is very important because this allows us discriminating between white noise and low $1/f$ noise. This general law can however be modified if the current induces itself modifications of the resistance or local heating. We have observed, in particular, in small GMR devices an increase of $1/f$ noise much faster than I^2.

GMR sensors have an isotropic dependence of the resistance unlike AMR where the signal is depending on the angle between field and current or Hall sensors where the voltage appears in a direction perpendicular to the current. Hence it is impossible to play on current direction to separate resistance variation and external field variation. This is a major issue with GMRs where spinning techniques used in Hall sensors or flipping of the current used in AMR sensors cannot be applied.

The second important point is the size effect on $1/f$ noise. Typically, PSD of the $1/f$ noise is decreasing as the volume of the sensor increases. This can be understood easily by an averaging effect. If we suppose that $1/f$ fluctuations are coming from small individual sources, you can consider that a resistance is the sum of N small resistances r so the total resistance $R = N \cdot r$ but the fluctuations of R are $\sqrt{N}$ larger than the individual r fluctuations. Hence for a given R, the fluctuations are decreasing as $\sqrt{N}$, i.e. as the square root of the volume. This has been observed in several systems for large enough sizes. At very small sizes an individual fluctuator may dominates and this rule is broken. There is a general phenomenological formula proposed by Hooge [40] which allows us to compare various sensors

$$S_V(\omega) = 2\pi \frac{\gamma_H V^2}{N_C \omega} = \frac{\gamma_H V^2}{N_C f} \tag{1.36}$$

where γ_H is a dimensionless constant. This formula is well adapted to semiconductors where the averaging is more on the number of carriers N_C than on the effective volume. For TMRs, the formula becomes:

$$S_V(\omega) = 2\pi \frac{\alpha V^2}{A\omega} = \frac{\alpha V^2}{Af} \tag{1.37}$$

where A is the active surface of the device and α is then a parameter with the dimension of a surface. This last formula describes rather correctly the evolution of the noise with the size of the sensors. We note that $1/f$ noise can exhibit a nonmagnetic and a magnetic component with sometimes different slopes.

The evolution of the noise as function of magnetic field can help to separate the two contributions. Often, the noise recorded under a strong field which saturates the different layers of a magnetic sensor is mainly nonmagnetic and an additional noise due to magnetic fluctuations in the layers appears in the sensitive regions. As described later, the shape of the sensors has a strong impact on the magnetic $1/f$ noise.

In case of TMRs, the $1/f$ noise depends also whether the junction is in the parallel or antiparallel state. In the parallel state, the number of channels opened through the barrier is larger than in the antiparallel state and hence the noise is smaller. This is a direct consequence of the reduction of the effective size of a junction.

1.7.4.2 Random Telegraph Noise

RTN or "popcorn" noise is the noise arising from the fluctuations of a specific source between two different levels. For magnetoresistive sensors, this noise generally appears in devices with a size small enough to let individual defects becoming dominant. However, it can be sometimes observed in reasonably large GMRs at high currents levels. RTN is, as explained before, a fluctuation between two levels with comparable energies and a barrier height able to give a typical characteristic time in the measurement range. Hence, RTN is very dependent on the temperature, field, and applied bias current.

RTN is difficult to handle and a sensor with RTN noise is in general very difficult to use even if it is theoretically possible to suppress partially this noise by data treatment. That suppression requires an RTN with a low fluctuation frequency and two states well separated. The treatment is then based on the recognition of each transition level from low state to high state and suppression of the step.

1.7.5 High Frequency Noise and Ferromagnetic Resonance

At high frequencies, the noise is usually dominated by thermal or shot noise. However, noise peaks can be detected in magnetoresistive sensors due to the fluctuations of magnetic layers. In the GHz regime, thin magnetic films present ferromagnetic resonances with frequencies dependent on the material and on the shape of the sensors. In small elements, quantization of the spin waves induces a large number of resonances. The noise detected is coming from two different sources. The first one is due to the GMR effect. The free layer is fluctuating with more important amplitude at resonance and if a DC current is sent in the device, a voltage at the resonance frequency appears. The second one is due to thermal and shot noises. This noise is amplified by the quality factor of the resonance and hence this appears as an extra noise even in the absence of bias current. The amplitude of this ferromagnetic resonance-enhanced noise might depend on the probing DC current due to spin transfer torque which affects the quality factor [41].

1.7.6 External Noise

With magnetic sensors, and, in particular very sensitive magnetic sensors, it is essential to take care of the magnetic external noise. Inside a laboratory, there are three types of external perturbations which lead to magnetic noise. First a number of discrete frequencies, including the power supply line (50/60 Hz) and its harmonics but also higher frequencies typically up to MHz coming from power supplies, low consumption lights, etc. All these lines correspond to real AC magnetic fields and hence are proportional to the bias current in the magnetoresistive sensor. The second source is a $1/f$ magnetic noise which exists everywhere. In a laboratory, this noise has an intensity of about 100 nT at 1 Hz and decreases slightly faster than $1/f$. In a good magnetic shielded room with passive and active shielding, the noise level at 1 Hz can be of the order of 100 fT.

The third type of noise is less intuitive. It is created by the vibration of the magnetoresistive sensor in an existing DC field. This noise can only be detected with very sensitive sensors, typically mounted with flux concentrators. The vibration induces a flux, the variation in a flux concentrator, and hence an additional signal. This noise can be easily recognized because it appears usually as bursts at fixed very low frequencies and their amplitude varies strongly when artificial vibrations are created.

1.7.7 Electronics and Noise Measurements

Noise is often difficult to measure quantitatively and there are several approaches to reliably estimate this quantity. Combining field and temperature variation can even complicate the measurement. In this part, we focus on a "standard" setup with some alternatives and with an emphasis on common errors.

1.7.7.1 Electronics Design

The electronics for a noise measurement or for interfacing magnetic sensors in an application can be separated roughly in five parts:

1) The sensor system which may contain one or several different sensors
2) A biasing source (voltage or current)
3) A front end electronics which contains a first preamplifier stage
4) An amplification, filtering, and shaping stage
5) An acquisition system

For noise measurements, the last two parts may be replaced by a spectrum analyzer. Figure 1.6 gives an overview of the electronics for typical noise measurements.

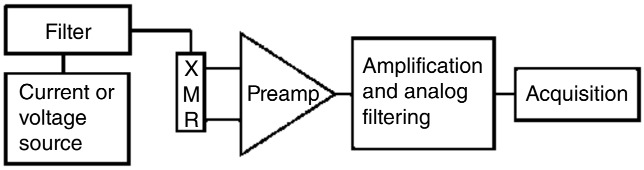

Figure 1.6 Schematics of electronics for typical noise measurements. *Source:* adapted from [32].

1.7.7.2 Connections Noise

In noise investigation as for the development of very sensitive magnetic sensors, it is necessary to take care of the connection quality. Often connections are made with wire bounding in Al or Au with an effective small surface contact. Even if the total resistance contact is small, a low frequency noise can appear. In addition, connector noise along a measurement chain can also be a source of noise which might not be negligible in the total noise if the sensor's noise is low.

1.7.7.3 Correlation for Preamplification Noise Suppression

When the signal of interest is small and dominated by the preamplification noise, it is difficult to measure it. A possible approach consists of using two preamplifiers which are measuring the same signal. If a cross-correlation as given in Eq. (1.18) is performed, we obtain the spectral density of the signal of interest plus three terms which are not correlated: the cross-correlation of the signal and each amplifier noise and the correlation between the noise of the two preamplifiers. By averaging, these three terms are reduced as the square root of the averaging number, but the spectral density is not reduced. Hence, with 100 averages the preamplification noise is reduced by 10. This can be applied for noise studies but not for applications.

References

1 Boll, R. and Overshott, K.J. (2008). *Sensors, Magnetic Sensors*. Wiley.
2 Meyer, H.W. (1971). *A History of Electricity and Magnetism*. Cambridgd, MA: The MIT Press.
3 Schubert, J. (1987). *Dictionary of Effects and Phenomena in Physics: Descriptions, Applications, Tables*. Wiley-VCH.
4 Acuña, M. (1974). Fluxgate magnetometers for outer planets exploration. *IEEE Transactions on Magnetics* 10 (3): 519–523.
5 Heidari, H. (2018). Electronic skins with a global attraction. *Nature Electronics* 1 (11): 578.

6 Williamson, S.J. and Kaufman, L. (1981). Biomagnetism. *Journal of Magnetism and Magnetic Materials* 22 (2): 129–201.
7 Parkinson, D.H. and Mulhall, B.E. (2013). *The Generation of High Magnetic Fields*. Springer.
8 Zijlstra, H. (1967). *Experimental Methods in Magnetism*. North-Holland Pub. Co.
9 Montgomery, D.B. (1969). *Solenoid Magnet Design*. Wiley.
10 Chen, C.-W. (2013). *Magnetism and Metallurgy of Soft Magnetic Materials*. Courier Corporation.
11 Heidari, H., Wacker, N., Roy, S., and Dahiya, R. (2015). Towards bendable CMOS magnetic sensors. In: *2015 11th Conference on PhD Research in Microelectronics and Electronics (PRIME)*, 314–317. IEEE.
12 Nabaei, V., Chandrawati, R., and Heidari, H. (2018). Magnetic biosensors: modelling and simulation. *Biosensors and Bioelectronics* 103: 69–86.
13 Heidari, H., Bonizzoni, E., Gatti, U., and Maloberti, F. (2014). A 0.18-μm CMOS current-mode hall magnetic sensor with very low bias current and high sensitive front-end. In: *SENSORS, 2014 IEEE*, 1467–1470. IEEE.
14 Heidari, H., Bonizzoni, E., Gatti, U. et al. (2016). CMOS vertical Hall magnetic sensors on flexible substrate. *IEEE Sensors Journal* 16 (24): 8736–8743.
15 Bentley, J.P. (1988). *Principles of Measurement Systems*. Pearson Education India.
16 Seippel, R.G. (1983). *Transducers, Sensors & Detectors*. Reston Pub. Co.
17 Korvink, J. and Paul, O. (2010). *MEMS: A Practical Guide of Design, Analysis, and Applications*. Springer Science & Business Media.
18 Middelhoek, S. and Audet, S.A. (1989). *Silicon Sensors*. Academic Press.
19 Sze, S.M. (1994). *Semiconductor Sensors*. New York: Wiley.
20 Roumenin, C.S. (1994). *Solid State Magnetic Sensors*. North-Hollande.
21 Bozorth, R.M. (1993). *Ferromagnetism*. by Richard M. Bozorth, pp. 992. ISBN 0-7803-1032-2. Wiley-VCH, August 1993. 1993 Aug:992.
22 Wohlfarth, E.P. and Buschow, K.H.J. (1980). *Ferromagnetic Materials: A Handbook on the Properties of Magnetically Ordered Substances*. Elsevier.
23 Tebble, R.S., Craik, D.J. (1969). *Magnetic Materials*. London: Wiley-Interscience; 1969 Nov 22.
24 Heck, C. (2013). *Magnetic Materials and Their Applications*. Elsevier.
25 Boll, R. (1979). *Soft Magnetic Materials: Fundamentals, Alloys, Properties, Products, Applications: The Vacuumschmelze Handbook*. Siemens.
26 Brignell, J.E., White, N.M., and Cranny, A.W.J. (1988). Sensor applications of thick-film technology. *IEE Proceedings I-Solid-State and Electron Devices* 135 (4): 77–84.
27 R. S. Popovic (1996). Hall effect devices (Adam Hilger, Bristol, 1991). *Google Scholar*, pp. 165–170
28 Roumenin, C. (1994). Functional magnetic-field microsensors: an overview (S & M 0144). *Sensors and Materials* 5: 285–285.

29 Roumenin, C.S. (1995). Magnetic sensors continue to advance towards perfection. *Sensors and Actuators A: Physical* 46 (1–3): 273–279.

30 Mohri, K., Uchiyama, T., and Panina, L.V. (1997). Recent advances of micro magnetic sensors and sensing application. *Sensors and Actuators A: Physical* 59 (1–3): 1–8.

31 Norton, H.N. (1990). *Sensor and Transducer Selection Guide*. Elsevier Advanced Technology.

32 Reig, C., Cardoso, S., and Mukhopadhyay, S.C. (2013). Giant magnetoresistance (GMR) sensors. *Ssmi6* 1: 157–180.

33 Johnson, J.B. (1927). Thermal agitation of electricity in conductors. *Nature* 119 (2984): 50.

34 Nyquist, H. (1928). Thermal agitation of electric charge in conductors. *Physical Review* 32 (1): 110.

35 Steinbach, A.H., Martinis, J.M., and Devoret, M.H. (1996). Observation of hot-electron shot noise in a metallic resistor. *Physical Review Letters* 76 (20): 3806.

36 Blanter, Y.M. and Büttiker, M. (2000). Shot noise in mesoscopic conductors. *Physics Reports* 336 (1–2): 1–166.

37 Guerrero, R., Aliev, F.G., Tserkovnyak, Y. et al. (2006). Shot noise in magnetic tunnel junctions: evidence for sequential tunneling. *Physical Review Letters* 97 (26): 266602.

38 Garzon, S., Chen, Y., and Webb, R.A. (2007). Enhanced spin-dependent shot noise in magnetic tunnel barriers. *Physica E: Low-Dimensional Systems and Nanostructures* 40 (1): 133–140.

39 Voss, R.F. and Clarke, J. (1976). Flicker (1/f) noise: equilibrium temperature and resistance fluctuations. *Physical Review B* 13 (2): 556.

40 Hooge, F.N. (1976). 1/f noise. *Physica B+C* 83 (1): 14–23.

41 Foros, J., Brataas, A., Bauer, G.E.W., and Tserkovnyak, Y. (2009). Noise and dissipation in magnetoelectronic nanostructures. *Physical Review B* 79 (21): 214407.